

# Structural relationship of curcumin derivatives binding to the BRCT domain of human DNA polymerase $\lambda$

Toshifumi Takeuchi<sup>1</sup>, Tomomi Ishidoh<sup>2</sup>, Hiroshi Iijima<sup>2</sup>, Isoko Kuriyama<sup>2</sup>, Noriko Shimazaki<sup>1</sup>, Osamu Koiwai<sup>1</sup>, Kouji Kuramochi<sup>1</sup>, Susumu Kobayashi<sup>3,4</sup>, Fumio Sugawara<sup>1,4</sup>, Kengo Sakaguchi<sup>1,4</sup>, Hiromi Yoshida<sup>2,5</sup> and Yoshiyuki Mizushima<sup>2,5,\*</sup>

<sup>1</sup>Department of Applied Biological Science, Tokyo University of Science, Noda, Chiba, Japan

<sup>2</sup>Department of Nutritional Science, Kobe-Gakuin University, Kobe, Hyogo, Japan

<sup>3</sup>Faculty of Pharmaceutical Sciences, Tokyo University of Science, Noda, Chiba, Japan

<sup>4</sup>Frontier Research Center for Genome and Drug Discovery, Tokyo University of Science, Noda, Chiba, Japan

<sup>5</sup>High Technology Research Center, Kobe-Gakuin University, Kobe, Hyogo, Japan

We previously reported that phenolic compounds, petasiphenol and curcumin (diferuloylmethane), were a selective inhibitor of DNA polymerase  $\lambda$  (pol  $\lambda$ ) *in vitro*. The purpose of this study was to investigate the molecular structural relationship of curcumin and 13 chemically synthesized derivatives of curcumin. The inhibitory effect on pol  $\lambda$  (full-length, i.e. intact pol  $\lambda$  including the BRCA1 C-terminal [BRCT] domain) by some derivatives was stronger than that by curcumin, and monoacetylcurcumin (compound 13) was the strongest pol  $\lambda$  inhibitor of all the compounds tested, achieving 50% inhibition at a concentration of 3.9  $\mu\text{M}$ . The compound did not influence the activities of replicative pols such as  $\alpha$ ,  $\delta$ , and  $\epsilon$ . It had no effect on pol  $\beta$  activity either, although the three-dimensional structure of pol  $\beta$  is thought to be highly similar to that of pol  $\lambda$ . Compound 13 did not inhibit the activity of the C-terminal catalytic domain of pol  $\lambda$  including the pol  $\beta$ -like core, in which the BRCT motif was deleted from its N-terminal region. MALDI-TOF MS analysis demonstrated that compound 13 bound selectively to the N-terminal domain of pol  $\lambda$ , but did not bind to the C-terminal region. Based on these results, the pol  $\lambda$ -inhibitory mechanism of compound 13 is discussed.

## Introduction

The human genome encodes 16 DNA polymerases (pols) to conduct cellular DNA synthesis (Bebenek & Kunkel 2004). Eukaryotic cells reportedly contain three replicative types; pols  $\alpha$ ,  $\delta$ , and  $\epsilon$ , mitochondrial pol  $\gamma$  and at least 12 repair types such as damaged DNA template synthesis; pols  $\beta$ ,  $\delta$ ,  $\epsilon$ ,  $\zeta$ ,  $\eta$ ,  $\theta$ ,  $\iota$ ,  $\kappa$ ,  $\lambda$ ,  $\mu$ ,  $\sigma$ , and REV1 (Friedberg *et al.* 2000). We have searched for natural compounds that selectively inhibit each of these eukaryotic pols to use as tools and molecular probes to distinguish pols and to clarify their biologic and *in vivo* functions (Mizushima *et al.* 1996, 1997, 1999, 2000, 2002a, 2003, 2004; Kuriyama *et al.* 2005). We reported on an interesting compound that selectively inhibits only

pol  $\lambda$  (Mizushima *et al.* 2002b). The natural compound was a phenolic compound, petasiphenol (compound 1), produced from a higher plant, a Japanese vegetable (*Petasites japonicus*), and the selectivity toward pol  $\lambda$  was extremely high. Then we found that another phenolic compound, curcumin (diferuloylmethane, compound 2), which is known as an antichronic inflammatory agent and an anti-oxidative compound (Sigma Reagent Catalog), is structurally similar to petasiphenol. Curcumin is a yellow substance from the root of the plant *Curcuma longa* Linn. Not unexpectedly, curcumin was also a potent pol  $\lambda$ -selective inhibitor. To our knowledge, there have been no reports about such natural inhibitors specific to X family pols, except for solanapyrone A as a pol  $\beta$  and  $\lambda$  inhibitor and prunasin as a pol  $\beta$  inhibitor, which we reported previously (Mizushima *et al.* 1999; Mizushima *et al.* 2002b). The compound differed from solanapyrone A in that it inhibited only pol  $\lambda$  among pols examined to date, and was a stronger pol  $\lambda$  inhibitor than solanapyrone A.

Communicated by: Fumio Hanaoka

\*Correspondence: E-mail: mizushin@nutr.kobegakuin.ac.jp

DOI: 10.1111/j.1365-2443.2006.00937.x

© 2006 The Author(s)

Journal compilation © 2006 by the Molecular Biology Society of Japan/Blackwell Publishing Ltd.

Genes to Cells (2006) 11, 223–235

223

Pol  $\lambda$  is a recently described eukaryotic pol belonging to the pol X family (Aoufouchi *et al.* 2000; Garcia-Diaz *et al.* 2000) comprising enzymes involved in DNA repair processes, whose main member is pol  $\beta$ . Human pol  $\lambda$  (63.4 kDa) consists of a nuclear transport signal (residues 1–35), a BRCA1 C-terminal (BRCT) domain (residues 36–132), a proline–serine-rich region (residues 133–243) and a pol  $\beta$ -like core region (residues 244–575). The N-terminal part of pol  $\lambda$  has similarity to yeast pol IV and contains a BRCT domain (Garcia-Diaz *et al.* 2000). The BRCT domain is present in several proteins involved in DNA repair and cell cycle checkpoint control (Bork *et al.* 1997; Zhang *et al.* 1998). Recently, it has been shown that the BRCT domain is involved in protein–protein interactions (Zhang *et al.* 1998). The C-terminal part of pol  $\lambda$  (residues 244–575) is composed of a catalytic core, which is similar to pol  $\beta$  (8-kDa domain and 31-kDa finger, palm and thumb polymerization domain) and has 32% amino acid identity to pol  $\beta$  (Garcia-Diaz *et al.* 2000). A truncated pol  $\lambda$ , in which the BRCT motif was deleted from the N-terminal region (i.e. the C-terminal region including the pol  $\beta$ -like core), has the pol activity (Garcia-Diaz *et al.* 2004).

In this study, we identified the structure of petasiphenol and curcumin essential to the inhibition of pol  $\lambda$ , and then chemically synthesized derivatives of curcumin. Some of the newly synthesized derivatives were stronger pol  $\lambda$  inhibitors than petasiphenol and curcumin. The same derivatives inhibited the activity of intact pol  $\lambda$ , but did not suppress the activity of the pol  $\lambda$ -catalytic core domain. Based on these results, the inhibitory action of the compound and its relation to the enzyme structure of pol  $\lambda$  will be discussed. These studies may help further clarify the structure and function of pol  $\lambda$  three-dimensionally and to synthesize a theoretically selective pol inhibitor.

## Results

### Effects of curcumin derivatives on the activity of DNA pol $\lambda$

As briefly described in the previous text, we reported that a phenolic compound, petasiphenol (compound 1 in Fig. 1), which was isolated from a Japanese vegetable (*P. japonicus*), is an inhibitor capable of selecting among the pols (Mizushina *et al.* 2002b). We investigated whether curcumin (compound 2 in Fig. 1), which is the same phenolic compound as petasiphenol and 13 chemically synthesized derivatives of curcumin (compounds 3–15 in Fig. 1), inhibited the activities of mammalian pols  $\alpha$ ,  $\beta$ , and  $\lambda$ . As shown in Fig. 2, 10  $\mu\text{M}$  of petasiphenol and

curcumin inhibited human pol  $\lambda$  activity. The inhibitory effect on pol  $\lambda$  by 10  $\mu\text{M}$  of compounds 4, 5, 13, and 14 was stronger than that by curcumin. As compounds 6–11, which do not have two enone moieties, did not influence the pol  $\lambda$  activity, the enone moiety might be important to the inhibition of pol  $\lambda$ . Petasiphenol has an enone moiety; therefore, one or more enone moieties in the compound might be essential for pol  $\lambda$  inhibition. Compounds 4, 5, and 13, which have an acetoxy moiety, strongly inhibited the activity of pol  $\lambda$ , and compound 13 (monoacetylcurcumin) was the strongest inhibitor among the compounds tested. The one acetoxy moiety at position C3' in compound 13 would stimulate the inhibitory effect on pol  $\lambda$ . On the other hand, none of the compounds inhibited the activities of calf pol  $\alpha$  and rat pol  $\beta$ .

### Effects of compound 13 on the activities of mammalian DNA pols and other DNA metabolic enzymes

Figure 3 shows the inhibition dose–response curves of compound 13 against mammalian pols. Compound 13 was effective at inhibiting human pol  $\lambda$  activity, and the inhibition was dose dependent, with 50% inhibition observed at a dose of 3.9  $\mu\text{M}$ . The compound had no influence at all on the activities of not only replicative pols such as calf pol  $\alpha$ , human pol  $\delta$ , and human pol  $\epsilon$ , or mitochondrial replicative pol such as human pols  $\gamma$ , but also repair-related pols such as rat pol  $\beta$  (Fig. 3). Compound 13 had no inhibitory effect on cauliflower (higher plant) pol I ( $\alpha$ -like) and II ( $\beta$ -like), prokaryotic pols such as the Klenow fragment of *Escherichia coli* pol I, *Taq* pol and T4 pol, and other DNA-metabolic enzymes such as calf DNA primase of pol  $\alpha$ , calf TdT, HIV-1 reverse transcriptase, T7 RNA pol, T4 polynucleotide kinase and bovine deoxyribonuclease I (Table 1). Therefore, compound 13 was a specific inhibitor of pol  $\lambda$  among the pols and DNA metabolic enzymes tested. Petasiphenol and curcumin also selectively inhibited the activity of pol  $\lambda$  (Table 1). The  $\text{IC}_{50}$  values in Table 1 did not change when the DNA template–primer was activated DNA (data not shown).

Interestingly, compound 13 selectively inhibited the activity of pol  $\lambda$ , which has been recently identified as a new member of the pol  $\beta$  family, and their three-dimensional structures are thought to be highly similar (Garcia-Diaz *et al.* 2000). Compound 13 did not inhibit the activity of either pol  $\beta$  or the C-terminal domain including pol  $\beta$ -like core region of pol  $\lambda$  (Fig. 3), indicating that it binds to the N-terminal region including the BRCT domain of pol  $\lambda$  directly, and subsequently,

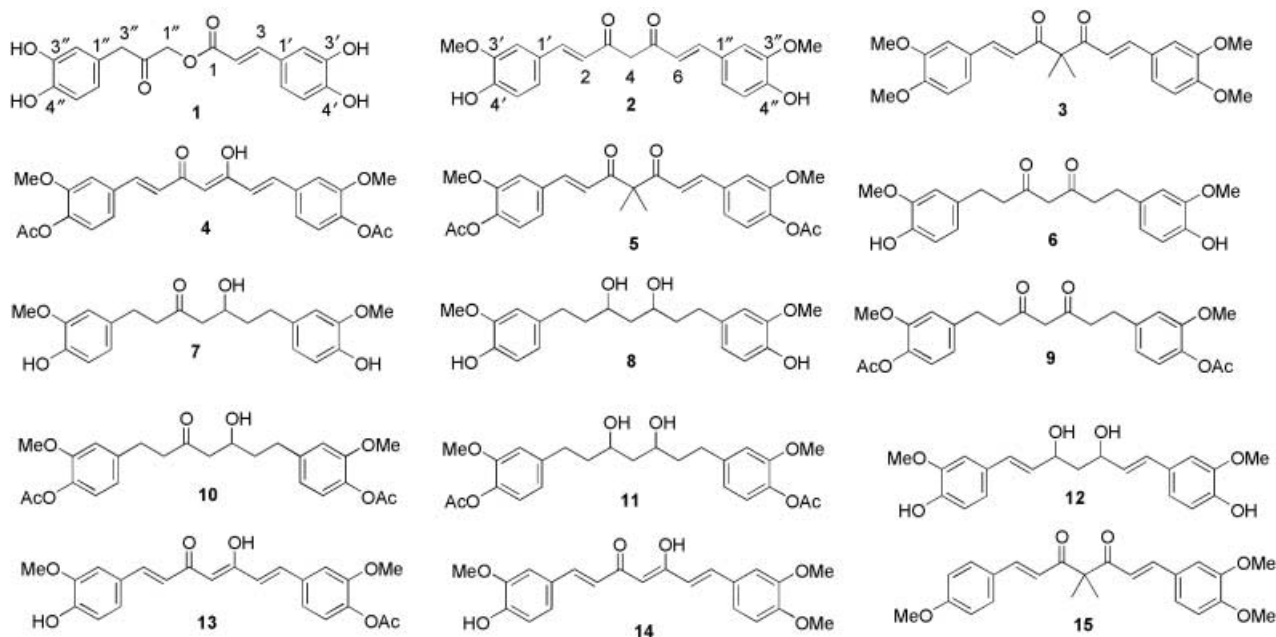


**Figure 1** Structure of curcumin derivatives. Compound 1: petasiphenol; compound 2: curcumin (diferuloylmethane); compound 3: (1*E*,6*E*)-1,7-bis(3',4'-dimethoxyphenyl)-4,4-dimethyl-1,6-heptadien-3,5-dione; compound 4: (1*E*,4*Z*,6*E*)-1,7-bis(4'-acetoxy-3'-methoxyphenyl)-5-hydroxy-1,4,6-heptatrien-3-one (diacetylcurcumin); compound 5: (1*E*,6*E*)-1,7-bis(4'-acetoxy-3'-methoxyphenyl)-4,4-dimethyl-1,6-heptadien-3,5-dione; compound 6: 1,7-bis(3'-hydroxy-4'-methoxyphenyl)-3,5-heptadiene; compound 7: 1,7-bis(3'-hydroxy-4'-methoxyphenyl)-5-hydroxy-3-heptanone; compound 8: 1,7-bis(3'-hydroxy-4'-methoxyphenyl)-3,5-heptadiol; compound 9: 1,7-bis(3'-acetoxy-4'-methoxyphenyl)-3,5-heptadione; compound 10: 1,7-bis(3'-acetoxy-4'-methoxyphenyl)-5-hydroxy-3-heptaone; compound 11: (1*E*,6*E*)-1,7-bis(3'-acetoxy-4'-methoxyphenyl)-3,5-dihydroxy-1,6-heptadiene; compound 12: (1*E*,6*E*)-1,7-bis(3'-hydroxy-4'-methoxyphenyl)-3,5-dihydroxy-1,6-heptadiene; compound 13: (1*E*,4*Z*,6*E*)-7-(4''-acetoxy-3''-methoxyphenyl)-5-hydroxy-1-(4'-hydroxy-3'-methoxyphenyl)hepta-1,4,6-trien-3-one (monoacetylcurcumin); compound 14: (1*E*,4*Z*,6*E*)-1-(3',4'-dimethoxyphenyl)-5-hydroxy-7-[4''-hydroxy-3''-methoxyphenyl]hepta-1,4,6-trien-3-one (monomethylcurcumin); compound 15: (1*E*,6*E*)-1-(3',4'-dimethoxyphenyl)-4-dimethyl-7-(4'-methoxyphenyl)hepta-1,6-trien-3,5-dione.

inhibited the activity of the C-terminal pol  $\beta$ -like core of pol  $\lambda$ . On the other hand, compound 13 did not inhibit the activity of TdT, which is also the X family enzyme with the BRCT domain (Table 1), suggesting that the compound did not always recognize any of the BRCT domain structure.

#### Inhibitory effect of compound 13 on 5'-phosphate recognition in DNA with gaps

Pol  $\beta$  consists of an independently folded N-terminal 8-kDa domain and C-terminal 31-kDa domain (Kumar *et al.* 1990a, 1990b). The N-terminal domain was found to possess binding specificity for the 5' phosphate in DNA with gaps, and cross-linking of pol  $\beta$  to such DNA is dependent on a 5'-phosphate moiety in the gap (Casas-Finet *et al.* 1991; Prasad *et al.* 1993, 1994). Because the binding of pol  $\beta$  was directed by the 8-kDa domain (Kumar *et al.* 1990a), it was suggested that the pol  $\beta$ -like

core region including the 8-kDa domain of pol  $\lambda$  could have the binding activity. To investigate the effect of compound 13 on the recognition by human pol  $\lambda$  of the 5' phosphate in DNA with gaps, a synthetic DNA substrate was formed by annealing two 17-residue oligonucleotides (designated primer 1 and primer 2) to a 39-residue template 1 creating a 5-nucleotide gap between the 3' hydroxyl of primer 1 and the 5' phosphate or 5' hydroxyl of primer 2 (see Fig. 4A and Experimental procedures). This DNA substrate was incubated with full-length pol  $\lambda$ , and then, the complex was photochemically cross-linked with UV light (Prasad *et al.* 1994). To score the covalently cross-linked complexes, the 5' end of the primer 1 oligonucleotide was separated by sodium dodecyl sulfate-polyacrylamide gel electrophoresis (SDS-PAGE), and the gel was analyzed by autoradiography (Fig. 4B). The results showed that the cross-linking among pol  $\lambda$ , template 1, and primer 1 was strongly influenced by the phosphate group at the 5' end of primer 2 (lanes 3 and

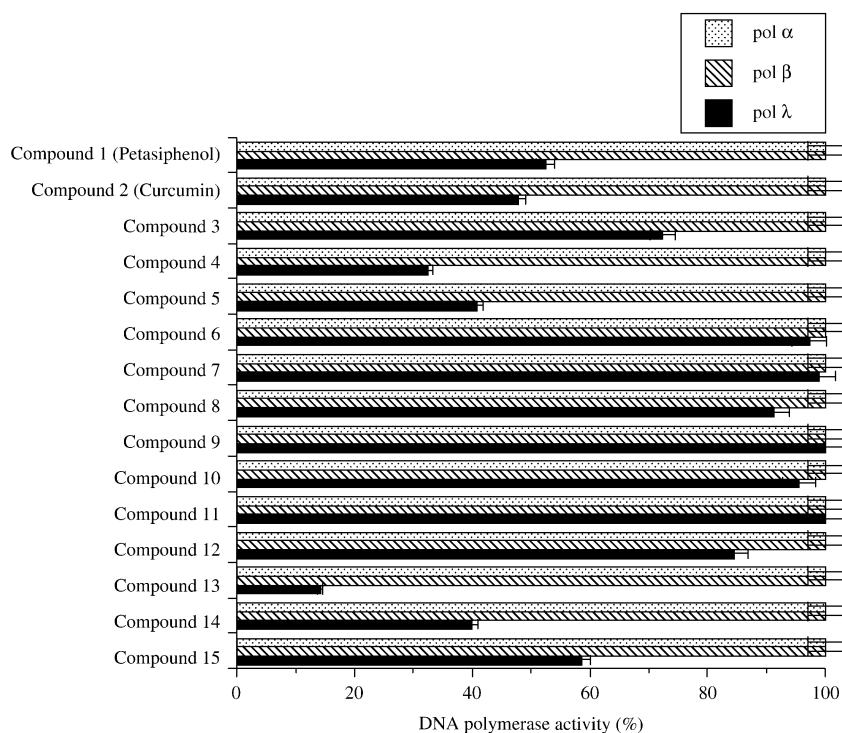


**Figure 2** Inhibitory effect of curcumin derivatives on the activities of mammalian DNA polymerases. The compounds (10  $\mu\text{M}$ ) were incubated with calf pol  $\alpha$ , rat pol  $\beta$  and human pol  $\lambda$  (0.05 units each). The enzymatic activity was measured as described in the text. Activity in the absence of compounds was taken as 100%. Data are shown as means  $\pm$  SEM for three independent experiments.

**Table 1**  $\text{IC}_{50}$  values of petasiphenol, curcumin and compound 13 for various DNA polymerases and other DNA metabolic enzymes

Enzyme	$\text{IC}_{50}$ value ( $\mu\text{M}$ )		
	Petasiphenol	Curcumin	Compound 13
Mammalian DNA pols			
Calf DNA pol $\alpha$	>100	>100	>100
Rat DNA pol $\beta$	>100	>100	>100
Human DNA pol $\gamma$	>100	>100	>100
Human DNA pol $\delta$	>100	>100	>100
Human DNA pol $\epsilon$	>100	>100	>100
Human DNA pol $\lambda$	$7.8 \pm 1.2$	$7.0 \pm 1.0$	$3.9 \pm 1.0$
Plant DNA pols			
Cauliflower DNA pol I ( $\alpha$ like)	>100	>100	>100
Cauliflower DNA pol II ( $\beta$ like)	>100	>100	>100
Prokaryotic DNA pols			
<i>E. coli</i> DNA pol I (Klenow fragment)	>100	>100	>100
<i>Taq</i> DNA pol	>100	>100	>100
T4 DNA pol	>100	>100	>100
Other DNA metabolic enzymes			
Calf DNA primase of DNA pol $\alpha$	>100	>100	>100
Calf terminal deoxynucleotidyl transferase	>100	>100	>100
HIV-1 reverse transcriptase	>100	>100	>100
T7 RNA pol	>100	>100	>100
T4 polynucleotide kinase	>100	>100	>100
Bovine deoxyribonuclease I	>100	>100	>100

These compounds were incubated with each enzyme (0.05 units). The enzymatic activity was measured as described in the Experimental section. Enzyme activity in the absence of the compound was taken as 100%.

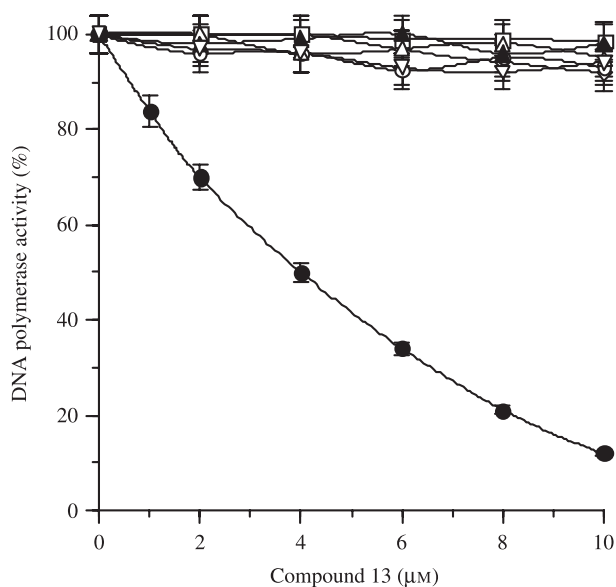


**Figure 3** Dose–response curves of compound 13. The enzymes used (0.05 units each) were calf pol  $\alpha$  (open square), rat pol  $\beta$  (open circle), human pol  $\gamma$  (open triangle), human pol  $\delta$  (open diamond), human pol  $\epsilon$  (open reverse-triangle), full-length human pol  $\lambda$  (residues 1–575) (closed circle) and the C-terminal domain including pol  $\beta$ -like core region of human pol  $\lambda$  (residues 133–575) (closed triangle). The pol activity was measured as described in the text. The pol activity in the absence of compound 13 was taken as 100%. Data are shown as means  $\pm$  SEM for three independent experiments.

4 in Fig. 4B). The molecular ratios of compound 13 and pol  $\lambda$  are shown as the inhibitor to protein ratio (I/P) in Fig. 4B. Even an excess amount of compound 13 (at an I/P ratio of more than 100) could not interfere with the recognition of the 5' phosphate by pol  $\lambda$  (lanes 7 and 8 in Fig. 4B). Compound 13 did not influence the activity on gapped DNA substrates of the C-terminal catalytic domain of pol  $\lambda$  either (data not shown).

#### Binding between compound 13 and the N-terminal BRCT domain or the C-terminal domain of DNA pol $\lambda$

It has been reported that some bioactive compounds containing an enone moiety bind their targets covalently (Kudo *et al.* 1999; Usui *et al.* 2004). Because the structure–activity relationships showed that an enone moiety is important for the inhibitory activity of the chemically synthesized curcumin derivatives against pol  $\lambda$  (Fig. 2), there is a possibility that curcumin derivatives such as compound 13 covalently bind human pol  $\lambda$  via enone moiety. To test this possibility, we investigated the change in

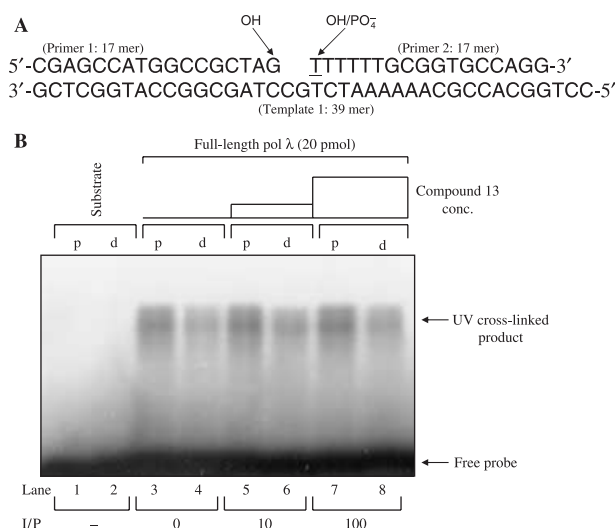


**Figure 4** 5'-Phosphate recognition in a 5-nucleotide gap by full-length pol  $\lambda$ . (A) Template 1, primer 1, and primer 2 were annealed as outlined under the Experimental section. (B) A photograph of an autoradiogram illustrating the result of UV cross-linking to a substrate with a 5-nucleotide gap is shown. Primer 2 (40 pmol in each lane) was either phosphorylated (p) (lanes 1, 3, 5, and 7) or not (d) (lanes 2, 4, 6, and 8) at its 5' end. The DNA substrate was mixed with full-length human pol  $\lambda$  and irradiated as described, and then, the cross-linked products were separated and analyzed as described under the Experimental section. The positions of the UV cross-linked product (pol  $\lambda$ /primer 1/template 1) and free probe are indicated. Lanes 3–8 contained pol  $\lambda$  at an amount of 20 pmol (1  $\mu$ M); lanes 1 and 2 contained no enzyme. Lanes 3, 4, 5, 6, 7, and 8 were each mixed with amounts of compound 13: 0, 0, 200, 200, 2000, and 2000 pmol, respectively. The concentration ratios of compound 13 (I) and pol  $\lambda$  (P) are indicated in the figure.

the molecular weight of human pol  $\lambda$  after compound 13 treatment by matrix-assisted laser desorption/ionization–time of flight (MALDI–TOF) mass spectrometry (Fig. 5). The molecular weight of full-length human pol  $\lambda$  was determined to be 68 350 (–cur), but that of compound 13-treated human pol  $\lambda$  was 68 758 (+cur) (Fig. 5A). The difference, 408, was thought to represent the molecular weight of compound 13 (M.W. 412). This binding is highly specific, because treatment with a fourfold excess molar amount of compound 13 resulted in an increase in mass corresponding to only one compound 13.

To determine which domain of pol  $\lambda$  was bound to compound 13, the N-terminal BRCT domain or the C-terminal catalytic domain, including the pol  $\beta$ -like core, these domains of pol  $\lambda$  were treated with compound 13 and then analyzed with MALDI–TOF mass spectrometry. The molecular weight of the BRCT domain of pol

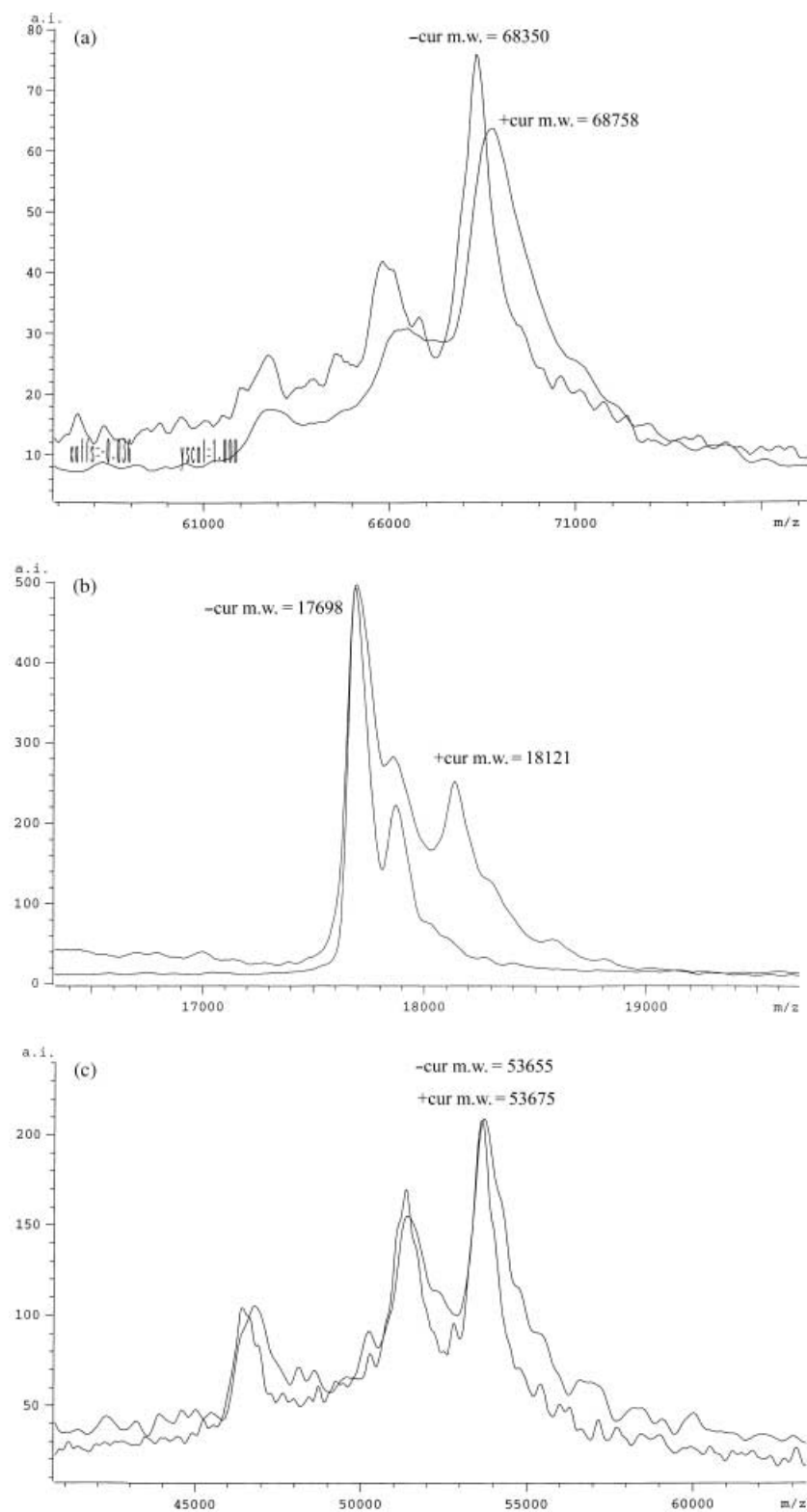


**Figure 5** MALDI-TOF MS analysis of the binding of compound 13 to human pol  $\lambda$ . (A) Full-length human pol  $\lambda$  (residues 1–575, M.W. 68 350) and compound 13-treated pol  $\lambda$ . (B) The N-terminal BRCT domain of human pol  $\lambda$  (residues 36–132, M.W. 17 698) and compound 13-treated the BRCT domain. (C) The C-terminal catalytic domain of human pol  $\lambda$  (residues 133–575, M.W. 53 655) and compound 13-treated the C-terminal domain.

$\lambda$  was determined to be 17 698 (–cur), but that of compound 13-treated human pol  $\lambda$  was 18 121 (–cur) (Fig. 5B). The difference, 423, was thought to represent the molecular weight of compound 13 (M.W. 412). However, there is no difference between the molecular weight of the C-terminal domain of pol  $\lambda$  and that of the compound 13-treated one (Fig. 5C). These results strongly suggest that compound 13 covalently binds the N-terminal BRCT domain of pol  $\lambda$ , but not the C-terminal catalytic domain including pol  $\beta$ -like core region.

### Simulation of the docking of the BRCT domain of human DNA pol $\lambda$ with compound 13

To confirm the previous assumption, we performed a homology modeling analysis of the BRCT domain of pol  $\lambda$ . As described in the early part of this report, compound 13 did not inhibit the activity of calf TdT, which contains a BRCT domain (Table 1), suggesting that the compound does not recognize the BRCT domain structure of TdT. Therefore, the three-dimensional structure of the BRCT domain of pol  $\lambda$  with or without compound 13 should be studied. At present, the BRCT domain structure of pol  $\lambda$  has not been determined by X-ray crystal or nuclear magnetic resonance analysis; however, the three-dimensional structures of the BRCT domains in human XRCC1 (PROTEIN DATA BANK [PDB] accession code: 1CDZ) (Garcia-Diaz *et al.* 2000), bacterial Nad<sup>+</sup>-dependent DNA ligase (PDB accession code: 1DGS) (Lee *et al.* 2000) and human DNA ligase IIIa (PDB accession code: 1IMO) (Krishnan *et al.* 2001) are available. The sequence of the BRCT domain of pol  $\lambda$  with 97 amino acids was retrieved from the databank in the National Center for Biotechnology Information (NCBI). The DNA sequence of the BRCT domain in human XRCC1 was used in this experiment because it was the most similar to that of human pol  $\lambda$  among the three proteins. From pairwise sequence alignments, the percent identity is 13% between the BRCT domains of human pol  $\lambda$  and human XRCC1. The multiple-sequence alignment of the template was obtained from the CD-SEARCH (NCBI), which compares a protein sequence against the conserved domain database with the RPS-BLAST program. The calculated three-dimensional structure of the BRCT domains of human pol  $\lambda$  is shown in Fig. 6A.

According to the homology modeling of the BRCT domain described previously, the three-dimensional binding structure between the BRCT domain of human pol  $\lambda$  and compound 13 was also studied. The N-terminal BRCT domain of pol  $\lambda$  (residues 36–132) was assumed to form four  $\alpha$ -helices and three  $\beta$ -sheets (Fig. 6A).

The three-dimensional position of the  $\alpha$ -helices in the BRCT domain of pol  $\lambda$  was different from that of human XRCC1, and the three-dimensional position of the  $\beta$ -sheets in the BRCT domain of pol  $\lambda$  was the same as that of human XRCC1 (Mizushina *et al.* 2002b). The compound 13-binding site of the modeled BRCT domain of human pol  $\lambda$  was refined using INSIGHT II/BINDING SITE ANALYSIS (Accelrys, San Diego, CA, USA). The data from the MALDI-TOF mass analysis suggested that a covalent bond is involved in the binding between compound 13 and the BRCT domain of human pol  $\lambda$  (Fig. 5B). A cavity having a space (i.e. the grid size, site of open size and site of cut-off size were 0.8 Å, 8 Å and 20 Å, respectively) where compound 13 can bind was searched for on the surface of the protein near Cys73 and Cys118, which can bind to the amino acid residues via covalent bonds. The number of final docking positions was only one, and a promising position including Cys73 was finally identified. Compound 13 did not inhibit the activity of TdT, which has a BRCT domain (Table 1). The BRCT domain sequence of pol  $\lambda$  was compared with that of TdT, and the conserved sequence region between pol  $\lambda$  and TdT was estimated. The cavity farthest away from the conserved region was determined as the compound 13-binding site.

As shown in Fig. 6B, the compound 13-binding region in the BRCT domain of human pol  $\lambda$  was assumed to consist of the  $\beta$ -sheet (Thr51 of sheet-1), the  $\alpha$ -helix (helix-1, residues 57–69) and the two loops (residues 51–56 and 70–75). Compound 13 could be mapped to one face of the BRCT domain of pol  $\lambda$ . The loop was significantly moved following the binding of compound 13 by the flexible docking procedure in the AFFINITY program within the INSIGHT II modeling software. The compound 13-interacted amino acid residues and their binding energies are indicated in Table 2. In the energy-minimized docking simulation, Cys73 in human pol  $\lambda$  forms a covalent bond with the position C1 in compound 13 (Fig. 6C,D). The binding energy between COO<sup>−</sup> of Glu59, COO<sup>−</sup> of Glu62 or NH<sub>4</sub><sup>+</sup> of Lys63 and the hydrophilic groups in compound 13 was −7.55664, −9.11299, or −37.93930 kcal/mol by hydrogen bonding, respectively (Fig. 6C,D), and the binding force consisted of coulomb forces (−3.35309, −3.93849, or −29.59488 kcal/mol, respectively) and van der Waals forces (−4.20355, −5.17450 or −8.34442 kcal/mol, respectively) (Table 2). The distances between the three hydroxyl groups of compound 13 and the hydrophilic residues of Glu59, Glu62, and Lys63 were 2.65, 2.74–2.87, and 2.43 Å, respectively (Fig. 6C). The binding energy between the other hydrophilic and neutral amino acids (i.e. Thr51 and Glu87) and compound 13 was

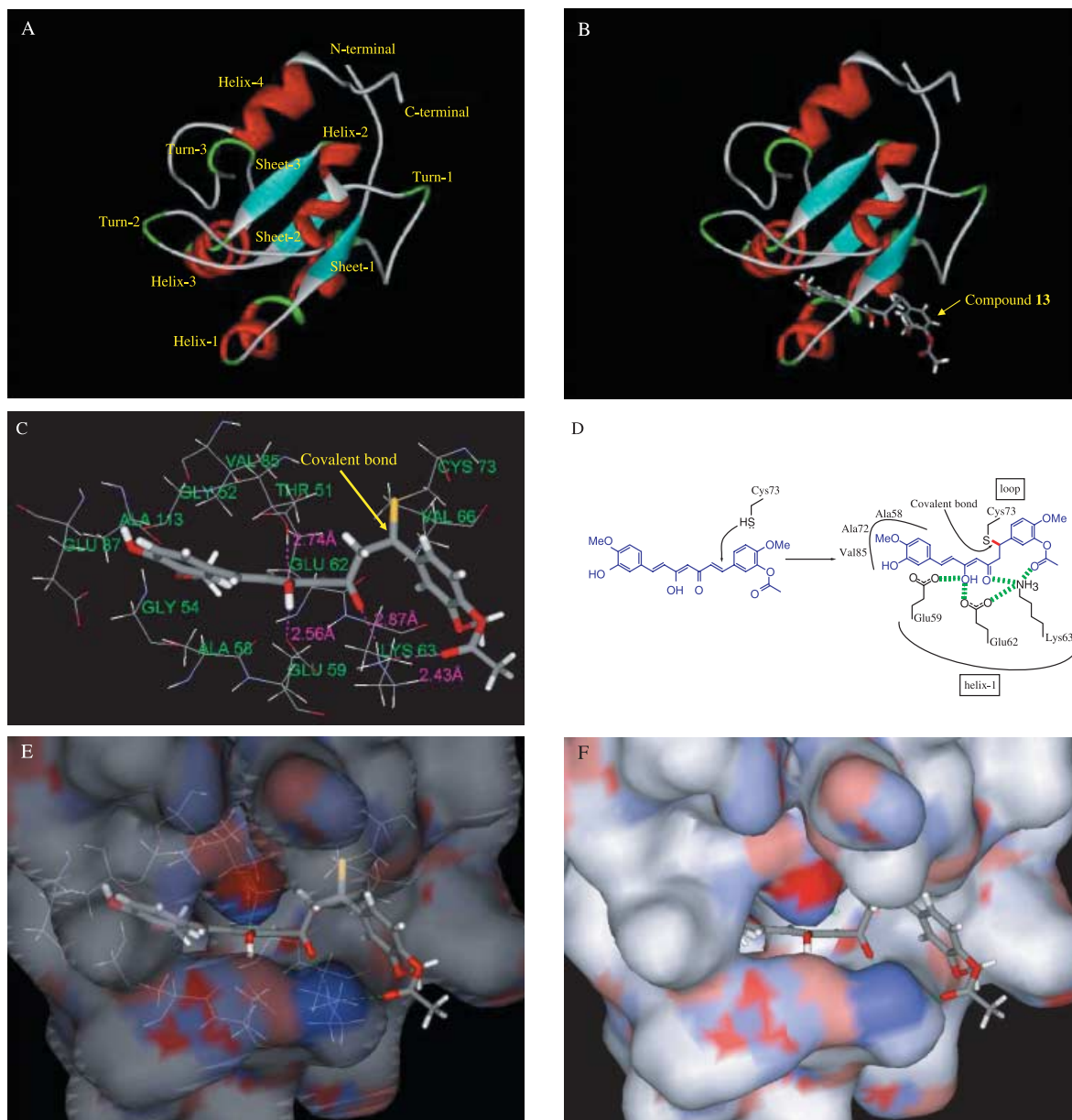


**Figure 6** Docking simulation of compound 13 interaction interface on the N-terminal BRCT domain of human pol  $\lambda$ . (A) The homology modeled structure of the N-terminal BRCT domain (97 amino acids, residues 36–132) of human pol  $\lambda$ . The colors of the three-dimensional structure of the domain consisting of  $\alpha$ -helix,  $\beta$ -sheet, turn, and flexible loop are red, white-blue, green, and white, respectively. (B) Flexible docking simulation of the BRCT domain of pol  $\lambda$  with compound 13. The colors of the three-dimensional structure of the domain consisting of  $\alpha$ -helix,  $\beta$ -sheet, turn, and flexible loop are red, white-blue, green, and white, respectively. (C) Interaction between compound 13 and amino acid residues of the BRCT domain of pol  $\lambda$ . (D) Chemical structure of compound 13 and the amino acid residues to which it binds. Compound 13 is blue. The colors of the covalent bond and five hydrogen bonds are red and green, respectively. (E, F) Connolly surface and electrostatic potential of the  $\beta$ -sheet (residues 49–51), the  $\alpha$ -helix (residues 57–69) and the two loops (residues 51–56 and 70–75) in the BRCT domain of pol  $\lambda$  with compound 13. Blue is positive charge, and red is negative charge. The three-dimensional structure of the N-terminal BRCT domain of human pol  $\lambda$  consists of four helices, helix 1 (residues 57–69), helix 2 (residues 99–106), helix 3 (residues 114–121), and helix 4 (residues 144–150), and three  $\beta$ -sheets (residues 49–51, 83–85, 109–111). The remainder of the domain consists of three turns (residues 79–80, 90–91, 128–131) and extended structures. The C $\alpha$ -backbone of the structure of pol  $\lambda$  is shown. The carbons, oxygens, hydrogens, and sulfurs of the structure of compound 13 and residues near compound are indicated in gray, red, white and yellow, respectively. This figure was prepared using INSIGHT II/DISCOVER (Accelrys).

**Table 2** The binding energy of compound 13 and DNA pol  $\lambda$ 

Compound 13-interacting Amino acid	Energy (kcal/mol)		
	Coulomb	van der Waals	Total
Thr51	-4.83848	-3.31812	-8.15661
Gly52	-0.22282	-2.25461	-2.47743
Gly54	-0.50666	-3.01302	-3.51968
Ala58	-2.01700	-4.29988	-6.31688
Glu59	-3.35309	-4.20355	-7.55664
Glu62	-3.93849	-5.17450	-9.11299
Lys63	-29.59488	-8.34442	-37.93930
Val66	0.30780	-2.09996	-1.79217
Val85	0.19016	-4.93938	-4.74922
Glu87	4.62628	-3.95713	0.66915
Ala113	-1.63004	-2.64235	-4.27239

All amino acids in the BRCT domain of human pol  $\lambda$ , which could interact with compound 13, are indicated. The binding energy was calculated by the flexible docking procedure in the AFFINITY program within the INSIGHT II modeling software.

-7.48746 kcal/mol, and the binding energy between the benzene backbone of compound 13 and the hydrophobic amino acids (i.e. Gly52, Gly54, Ala58, Val66, Val85, and Ala113) was -23.12777 kcal/mol (Table 2). The Connolly surface of the loops and the three-dimensional position of compound 13 are indicated in Fig. 6E,F. On the BRCT domain of pol  $\lambda$ , compound 13 was smoothly intercalated into the pocket of the loops, and the side of the nonacetoxy group on compound 13 (the left side of compound 13 in Fig. 6E,F) just fitted into the pocket of the BRCT domain. The residues around the amino acid site consisting of a covalent bond (i.e. Cys73) and five hydrogen bonds (i.e. Glu59, Glu62 and Lys63) appear to be important for binding to compound 13.

## Discussion

This is the first report of the characterization of an inhibitor specific to a mammalian pol. Of the newly synthesized compounds, compound 13 (monoacetylcurcumin) was the strongest inhibitor of human pol  $\lambda$  at a concentration of 1–10  $\mu$ M. Because the specificity was extremely high, compound 13 could be useful as a pol  $\lambda$ -specific inhibitor in studies to determine the precise roles of pol  $\lambda$ . Compound 13 must inhibit pol  $\lambda$  activity indirectly by acting at the BRCT domain. It is possible that compound 13 might inhibit other cellular proteins containing the BRCT domain, for example, TdT. Compound 13, however, did not influence the activity of TdT at all (Table 1). Compound 13 could not recognize the BRCT domain of TdT, suggesting that the three-

dimensional structure of the domain differs between pol  $\lambda$  and TdT, and subsequently, compound 13 could selectively inhibit pol  $\lambda$ .

Although the biochemical function of pol  $\lambda$  is unclear as yet, pol  $\lambda$  appears to act in a similar manner to pol  $\beta$  (Garcia-Diaz *et al.* 2002). Pol  $\beta$ , which is widely recognized to have a role in the short-patch base excision repair (BER) pathway (Singhal & Wilson 1993; Sobol *et al.* 1996; Garcia-Diaz *et al.* 2001; Garcia-Diaz *et al.* 2002; Ramadan *et al.* 2002), is essential for neural development (Sugo *et al.* 2000). Recently, pol  $\lambda$  was found to have dRP lyase activity, but not AP lyase activity (Garcia-Diaz *et al.* 2001), and to be able to substitute for pol  $\beta$  in *in vitro* BER, suggesting that pol  $\lambda$  also participates in BER. Northern blot analysis indicated that the transcript of pol  $\beta$  was abundantly expressed in the testis, thymus, and brain in rats (Hirose *et al.* 1989), but pol  $\lambda$  was transcribed mostly in the testis (Garcia-Diaz *et al.* 2000). A reason why the testis and thymus require pol  $\beta$  activity has been suggested: both organs have DNA repair and recombination systems for meiotic crossing over and immunoglobulin production (Plug *et al.* 1997; Esposito *et al.* 2000), and the systems require the pol. The roles of pol  $\beta$  in the brain are unknown as yet. Therefore, pol  $\lambda$  as well as pol  $\beta$  may also have a role in the testis. Because the DNA repair system at meiotic prophase requires pol  $\beta$  activity, the system must contain a process similar to BER. The system may also require pol  $\lambda$  activity. However, speculation concerning the biochemistry, structure, and function of pol  $\lambda$  should be done later, because the *in vivo* function is mostly unknown. We are at present analyzing the structure and function of pol  $\lambda$  using an inhibitor.

As described previously, another purpose of this study was to screen for a useful agent for analyzing the *in vivo* functions of pol  $\beta$  and pol  $\lambda$  in pol  $\beta$ - and pol  $\lambda$ -rich tissues. We could report the properties of compound 13 with regard to its effect on pol  $\lambda$ . Although pol  $\beta$  was efficiently transcribed in the testis, the thymus and the brain, pol  $\lambda$  was mainly expressed in the testis (Garcia-Diaz *et al.* 2000). Because solanapyrone A could inhibit the activities of both pol  $\beta$  and pol  $\lambda$  and compound 13 could distinguish between pol  $\beta$  and pol  $\lambda$ , compound 13 and solanapyrone A would be useful for analyzing the function of pol  $\beta$  and pol  $\lambda$  in the testis, especially at the point where homologous chromosomes pair and recombine during the meiotic prophase. Higher plants have no pol  $\beta$ , but pol  $\lambda$  (Uchiyama *et al.* 2004). Moreover, the activity of the plant pol  $\lambda$  is present only in cells at the meiotic prophase (Uchiyama *et al.* 2004). These natural compounds may therefore act on the plant reproductive system.

It has been shown that the BRCT domain of pol  $\lambda$  is involved in interaction with nonhomologous end-joining (NHEJ) factors (Lee *et al.* 2004), and therefore, it can be predicted that compound 13 inhibits the capacity of pol  $\lambda$  to participate in an NHEJ mechanism. Moreover, as speculated, compound 13 may lead block the mismatch error in DNA repair synthesis to rescue cells containing damaged DNA during clinical radiation therapy or chemotherapy. Curcumin derivatives such as compound 13 could be a useful molecular tool for developing a drug design strategy for cancer chemotherapy agents to help with clinical radiation therapy or cancer chemotherapy.

## Experimental procedures

### Materials

Nucleotides and chemically synthesized DNA template-primers such as poly(dA), poly(rA) and oligo(dT)<sub>12-18</sub>, and [<sup>3</sup>H]-2'-deoxythymidine 5' triphosphate (dTTP, 43 Ci/mmol) were purchased from Amersham Biosciences (Buckinghamshire, UK). All other reagents were of analytical grade and were purchased from Nakarai Tesque (Kyoto, Japan).

### Enzymes

Pol  $\alpha$  was purified from calf thymus by immunoaffinity column chromatography (Tamai *et al.* 1988). Recombinant rat pol  $\beta$  was purified from *Escherichia coli* JMp $\beta$ 5 as described by Date *et al.* (1988). The human pol  $\gamma$  catalytic gene was cloned into pFastBac. The histidine-tagged enzyme was expressed using a BAC-TO-BAC HT Baculovirus Expression System according to the supplier's manual (Life Technologies, MD) and purified using Pro-Boundresin (Invitrogen Japan, Tokyo, Japan). Human pol  $\delta$  and  $\epsilon$

were purified from the nuclear fraction of human peripheral blood cancer cells (Molt-4) using the second subunit of pol  $\delta$ - and  $\epsilon$ -conjugated affinity column chromatography, respectively (Oshige *et al.* 2004). The cDNA encoding full-length human pol  $\lambda$  (residues 1-575, 68.4 kDa), the N-terminal BRCT domain of pol  $\lambda$  (residues 36-132, 17.7 kDa) and the C-terminal catalytic domain of pol  $\lambda$  lacking the BRCT domain (i.e. pol  $\beta$ -like core region, residues 245-575, 53.7 kDa) were generated by polymerase chain reaction (PCR) using the primers L-F1 (5'-GCAGAATTCATGGATCCCAGGGGTATCTTGAAG-3') and L-R1 (5'-GTTCTCGAGCCAGTCCCGCTCAGCAGGTTCTCG-3'), L-F4 (5'-GCAGAATTCGTACTIONTTCGCAAAGATTCCTAGGAGG-3') and L-R4 (5'-CCAAAGCTTGATGCTGAATCCAGCTACATCCAC-3'), and L-F3 (5'-CGGGAATTCCTCATCCCCAGTAGGTACTIONTTCGCAAAGATTCCTAGGAGG-3') and LR-1, respectively, and then constructed and purified as previously described (Mizushina *et al.* 2002b; Shimazaki *et al.* 2002). Pol I ( $\alpha$ -like) and II ( $\beta$ -like) from a higher plant, cauliflower inflorescence, were purified according to the methods outlined by Sakaguchi *et al.* (1980). The Klenow fragment of pol I and human immunodeficiency virus type 1 (HIV-1) reverse transcriptase were purchased from Worthington Biochemical (Freehold, NJ, USA). Calf thymus TdT, T7 RNA pol and bovine pancreas deoxyribonuclease I were purchased from Stratagene Cloning Systems (La Jolla, CA, USA). *Taq* pol, T4 pol and T4 polynucleotide kinase were purchased from Takara (Tokyo, Japan).

### DNA polymerase assays

The reaction mixtures for pol  $\alpha$ , pol  $\beta$ , plant pols and prokaryotic pols were previously described (Mizushina *et al.* 1996, 1997). Those for pol  $\gamma$ ,  $\delta$ , and  $\epsilon$  were as described by Ogawa *et al.* (1998). The reaction mixture for pol  $\lambda$  was the same as that for pol  $\beta$ . The substrates of the pols used were poly(dA)/oligo(dT)<sub>12-18</sub> and dTTP as the DNA template primer and nucleotide substrate, respectively. The substrates of HIV-1 reverse transcriptase used were poly(rA)/oligo(dT)<sub>12-18</sub> and dTTP as template primer and nucleotide substrate, respectively. The substrates of TdT used were oligo(dT)<sub>12-18</sub> (3'-OH) and dTTP as template primer and nucleotide substrate, respectively. The compounds were dissolved in dimethylsulfoxide (DMSO) at various concentrations and sonicated for 30 s. The sonicated samples (4  $\mu$ L) were mixed with 16  $\mu$ L of each enzyme (final 0.05 units) in 50 mM Tris-HCl (pH 7.5) containing 1 mM dithiothreitol, 50% glycerol, and 0.1 mM ethylenediaminetetraacetic acid (EDTA), and kept at 0 °C for 10 min. These inhibitor-enzyme mixtures (8  $\mu$ L) were added to 16  $\mu$ L of each of the standard enzyme reaction mixtures, and incubation was carried out at 37 °C for 60 min, except for *Taq* pol, which was incubated at 74 °C for 60 min. The activity without the inhibitor was considered to be 100%, and the remaining activity at each concentration of inhibitor was determined relative to this value. One unit of pol activity was defined as the amount of enzyme that catalyzed the incorporation of 1 nmol of deoxyribonucleotide triphosphate (i.e. dTTP) into the synthetic DNA template-primers (i.e. poly(dA)/oligo(dT)<sub>12-18</sub>, A/T = 2/1) in 60 min at 37 °C under normal reaction conditions for each enzyme (Mizushina *et al.* 1996, 1997).

### Other enzyme assays

Activities of calf DNA primase of pol  $\alpha$ , T7 RNA pol, T4 polynucleotide kinase, and bovine deoxyribonuclease I were measured in each of the standard assays according to the manufacturer's specifications as described by Tamiya-Koizumi *et al.* (1997), Nakayama & Saneyoshi (1985), Soltis & Uhlenbeck (1982), and Lu & Sakaguchi (1991), respectively.

### 5' and 3' end labeling

The 5' end of the dephosphorylated primer (Primer 1; 17 mer, in Fig. 4A) was labeled with T4 polynucleotide kinase using [ $\gamma$ - $^{32}$ P]-ATP as previously described (Sambrook *et al.* 1989). These oligonucleotides were annealed to their complementary strands by heating the solution at 90 °C for 3 min, followed by slow cooling to 25 °C. The  $^{32}$ P-labeled duplex oligodeoxynucleotide was separated from unincorporated [ $\gamma$ - $^{32}$ P]-ATP using a MicroSpin G-25 column (Amersham Pharmacia Biotech) according to the manufacturer's suggested protocol.

### UV cross-linking to DNA

Human pol  $\lambda$  (20 pmol = 1  $\mu$ M) was mixed with the 5-nucleotide gapped DNA template-primer (0.5  $\mu$ M) (Doherty *et al.* 1996) and various concentrations of compound 13 in a reaction mixture containing 20 mM Tris-HCl (pH 8.0), 20 mM NaCl, 1 mM EDTA, 5 mM MgCl<sub>2</sub>, and 10% DMSO, and incubated at room temperature for 15 min. The samples were spotted onto Parafilm and irradiated at 254 nm for 4 min using a UV-Stratalinker (Stratagene Cloning Systems). The photochemical cross-linked 68.4-kDa protein of full-length pol  $\lambda$ -DNA complexes were separated by 15% SDS-PAGE and visualized by autoradiography.

### MALDI-TOF mass analysis

Full-length human pol  $\lambda$  (2  $\mu$ M), the N-terminal BRCT domain of human pol  $\lambda$  (6  $\mu$ M) or the C-terminal catalytic domain of human pol  $\lambda$  (4  $\mu$ M) were mixed with four equivalents of compound 13 at room temperature. The MALDI analyses were performed using a reflex III MALDI-TOF mass spectrometer (Bruker Daltonics, Billerica, MA, USA). A saturated MALDI matrix solution (0.5  $\mu$ L) of sinapinic acid in 1 : 1 MeCN : water and 0.5  $\mu$ L of sample solution were spotted onto the MALDI target. Co-crystallization of the sample and matrix was allowed to proceed at room temperature.

### Protein-inhibitor docking modeling

The generation of the N-terminal BRCT domain of human pol  $\lambda$  was performed using the molecular modeling software INSIGHT II/HOMOLOGY (Accelrys). All calculations were conducted on an HP workstation wx4100 (3.4GHz processor and 1024MB of memory), running under the Red Hat Enterprise Linux WS2.1 operating system. The BRCT domain of pol  $\lambda$  was refined based

on molecular dynamic simulations using INSIGHT II/DISCOVER (Accelrys). The binding site of compound 13 on the BRCT domain of human pol  $\lambda$  was determined using the software INSIGHT II/BINDING SITE ANALYSIS (Accelrys), and the molecular docking of the compound and the protein was modeled using a flexible docking procedure in the discovery program within the INSIGHT II modeling software (Accelrys). The calculations used a CVFF force field in the discovery program.

### Acknowledgements

We are grateful to Dr M. Takemura of Mie University and Dr A. Matsukage of Japan Women's University for preparing calf pol  $\alpha$  and rat pol  $\beta$ , respectively. This work was supported in part by a Grant-in-Aid for Kobe Gakuin University Joint Research (A) (H.Y. and Y.M.) and "High-Tech Research Center" Project for Private Universities: matching fund subsidy from MEXT (Ministry of Education, Culture, Sports, Science and Technology), 2001–2005 (H.Y. and Y.M.). Y.M. acknowledges Grants-in-Aid from the Takeda Science Foundation (Japan), the Mochida Memorial Foundation for Medical and Pharmaceutical Research (Japan), the Japan Food Chemical Research Foundation (Japan) and Grant-in-Aid 16710161 for Scientific Research, MEXT (Japan).

### References

- Aoufouchi, S., Flatter, E., Dahan, A., *et al.* (2000) Two novel human and mouse DNA polymerases of the polX family. *Nucleic Acids Res.* **28**, 3684–3693.
- Bebenek, K. & Kunkel, T.A. (2004) Functions of DNA polymerases. *Adv. Protein Chem.* **69**, 137–165.
- Bork, P., Hofmann, K., Bucher, P., Neuwald, A.F., Altschul, S.F. & Koonin, E.V. (1997) A superfamily of conserved domains in DNA damage-responsive cell cycle checkpoint proteins. *FASEB J.* **11**, 68–76.
- Casas-Finet, J.R., Kumar, A., Morris, G., Wilson, S.H. & Karpel, R.L. (1991) Spectroscopic studies of the structural domains of mammalian DNA  $\beta$ -polymerase. *J. Biol. Chem.* **266**, 19618–19625.
- Date, T., Yamaguchi, M., Hirose, F., *et al.* (1988) Expression of active rat DNA polymerase  $\beta$  in *Escherichia coli*. *Biochemistry* **27**, 2983–2990.
- Doherty, A.J., Serpell, L.C. & Ponting, C.P. (1996) The helix-hairpin-helix DNA-binding motif: a structural basis for non-sequence-specific recognition of DNA. *Nucleic Acids Res.* **24**, 2488–2497.
- Esposito, G., Texido, G., Betz, U.A.K., *et al.* (2000) Mice reconstituted with DNA polymerase  $\beta$ -deficient fetal liver cells are able to mount a T-cell-dependent immune response and mutate their Ig genes normally. *Proc. Natl. Acad. Sci. USA* **97**, 1166–1171.
- Friedberg, E.C., Feaver, W.J. & Gerlach, V.L. (2000) The many faces of DNA polymerases: strategies for mutagenesis and for mutational avoidance. *Proc. Natl. Acad. Sci. USA* **97**, 5681–5683.
- Garcia-Diaz, M., Bebenek, K., Krahn, J.M., Blanco, L., Kunkel, T.A. & Pedersen, L.C. (2004) A structural solution for the DNA

- polymerase 1-dependent repair of DNA gaps with minimal homology. *Mol. Cell* **13**, 561–572.
- Garcia-Diaz, M., Bebenek, K., Kunkel, T.A. & Blanco, L. (2001) Identification of an intrinsic 5'-deoxyribose-5-phosphate lyase activity in human DNA polymerase 1: a possible role in base excision repair. *J. Biol. Chem.* **276**, 34659–34663.
- Garcia-Diaz, M., Bebenek, K., Sabariego, R., *et al.* (2002) DNA polymerase 1, a novel DNA repair enzyme in human cells. *J. Biol. Chem.* **277**, 13184–13191.
- Garcia-Diaz, M., Dominguez, O., Lopez-Fernandez, L.A., *et al.* (2000) DNA polymerase 1 (Pol  $\lambda$ ), a novel eukaryotic DNA polymerase with a potential role in meiosis. *J. Mol. Biol.* **301**, 851–867.
- Hirose, F., Hotta, Y., Yamaguchi, M. & Matsukage, A. (1989) Difference in the expression level of DNA polymerase  $\beta$  among mouse tissues: high expression in the pachytene spermatocyte. *Exp. Cell Res.* **181**, 169–180.
- Krishnan, V.V., Thornton, K.H., Thelen, M.P. & Cosman, M. (2001) Solution structure and backbone dynamics of the human DNA ligase III $\alpha$  BRCT domain. *Biochemistry* **40**, 13158–13166.
- Kudo, N., Matsumori, N., Taoka, H., *et al.* (1999) Leptomycin B inactivates CRM1/exportin 1 by covalent modification at a cysteine residue in the central conserved region. *Proc. Natl. Acad. Sci. USA* **96**, 9112–9117.
- Kumar, A., Abbotts, J., Karawya, E.M. & Wilson, S.H. (1990a) Identification and properties of the catalytic domain of mammalian DNA polymerase  $\beta$ . *Biochemistry* **29**, 7156–7159.
- Kumar, A., Widen, S.G., Williams, K.R., *et al.* (1990b) Studies of the domain structure of mammalian DNA polymerase  $\beta$ : identification of a discrete template binding domain. *J. Biol. Chem.* **265**, 2124–2131.
- Kuriyama, I., Asano, N., Kato, I., *et al.* (2005) Dipeptide alcohol-based inhibitors of eukaryotic DNA polymerase  $\alpha$ . *Bioorg. Med. Chem.* **13**, 2187–2196.
- Lee, J.W., Blanco, L., Zhou, T., *et al.* (2004) Implication of DNA polymerase 1 in alignment-based gap filling for nonhomologous DNA end joining in human nuclear extracts. *J. Biol. Chem.* **279**, 805–811.
- Lee, J.Y., Chang, C., Song, H.K., *et al.* (2000) Crystal structure of NAD(+)-dependent DNA ligase: modular architecture and functional implications. *EMBO J.* **19**, 1119–1129.
- Lu, B.C. & Sakaguchi, K. (1991) An endo-exonuclease from meiotic tissues of the basidiomycete *Coprinus cinereus*: its purification and characterization. *J. Biol. Chem.* **266**, 21060–21066.
- Mizushina, Y., Kamisuki, S., Kasai, N., *et al.* (2002a) A plant phytoxin, solanapyrone A, is an inhibitor of DNA polymerase beta and 1. *J. Biol. Chem.* **277**, 630–638.
- Mizushina, Y., Kamisuki, S., Kasai, N., *et al.* (2002b) Petasiphenol: a DNA polymerase 1 inhibitor. *Biochemistry* **41**, 14463–14471.
- Mizushina, Y., Kamisuki, S., Mizuno, T., *et al.* (2000) Dehydroaltenuin, a mammalian DNA polymerase  $\alpha$  inhibitor. *J. Biol. Chem.* **275**, 33957–33961.
- Mizushina, Y., Kasai, N., Miura, K., *et al.* (2004) Structural relationship of lithocholic acid derivatives binding to the N-terminal 8-kDa domain of DNA polymerase  $\beta$ . *Biochemistry* **41**, 10669–10677.
- Mizushina, Y., Takahashi, N., Ogawa, A., *et al.* (1999) The cyanogenic glucoside, prunasin (D-mandelonitrile- $\beta$ -D-glucoside), is a novel inhibitor of DNA polymerase  $\beta$ . *J. Biochem. (Tokyo)* **126**, 430–436.
- Mizushina, Y., Tanaka, N., Yagi, H., *et al.* (1996) Fatty acids selectively inhibit eukaryotic DNA polymerase activities *in vitro*. *Biochim. Biophys. Acta* **1308**, 256–262.
- Mizushina, Y., Yoshida, S., Matsukage, A. & Sakaguchi, K. (1997) The inhibitory action of fatty acids on DNA polymerase  $\beta$ . *Biochim. Biophys. Acta* **1336**, 509–521.
- Mizushina, Y., Xu, X., Asahara, H., *et al.* (2003) A sulphoquinovosyl diacylglycerol is a DNA polymerase  $\epsilon$  inhibitor. *Biochem. J.* **370**, 299–305.
- Nakayama, C. & Saneyoshi, M. (1985) Inhibitory effects of 9- $\beta$ -D-xylofuranosyladenine 5'-triphosphate on DNA-dependent RNA polymerase I and II from cherry salmon (*Oncorhynchus masou*). *J. Biochem. (Tokyo)* **97**, 1385–1389.
- Ogawa, A., Murate, T., Suzuki, M., Nimura, Y. & Yoshida, S. (1998) Lithocholic acid, a putative tumor promoter, inhibits mammalian DNA polymerase  $\beta$ . *Jpn. J. Cancer Res.* **89**, 1154–1159.
- Oshige, M., Takeuchi, R., Ruike, R., Kuroda, K. & Sakaguchi, K. (2004) Subunit protein-affinity isolation of Drosophila DNA polymerase catalytic subunit. *Protein Expr. Purif.* **35**, 248–256.
- Plug, A.W., Clairmont, C.A., Sapi, E., Ashley, T. & Sweasy, J.B. (1997) Evidence for a role for DNA polymerase  $\beta$  in mammalian meiosis. *Proc. Natl. Acad. Sci. USA* **94**, 1327–1331.
- Prasad, R., Beard, W.A. & Wilson, S.H. (1994) Studies of gapped DNA substrate binding by mammalian DNA polymerase  $\beta$ : dependence on 5'-phosphate group. *J. Biol. Chem.* **269**, 18096–18101.
- Prasad, R., Kumar, A., Widen, S.G., Casas-Finet, J.R. & Wilson, S.H. (1993) Identification of residues in the single-stranded DNA-binding site of the 8-kDa domain of rat DNA polymerase  $\beta$  by UV cross-linking. *J. Biol. Chem.* **268**, 22746–22755.
- Ramadan, K., Shevelev, I.V., Maga, G. & Hubscher, U. (2002) DNA polymerase 1 from calf thymus preferentially replicates damaged DNA. *J. Biol. Chem.* **277**, 18454–18458.
- Sakaguchi, K., Hotta, Y. & Stern, H. (1980) Chromatin-associated DNA polymerase activity in meiotic cells of lily and mouse. *Cell Struct. Funct.* **5**, 323–334.
- Sambrook, J., Fritsch, E.F. & Maniatis, T. (1989) *Molecular Cloning: a Laboratory Manual*, 2nd edn, pp. 11–31. Cold Spring Harbor, NY: Cold Spring Harbor Laboratory Press.
- Shimazaki, N., Yoshida, K., Kobayashi, T., Toji, S., Tamai, T. & Koiwai, O. (2002) Over-expression of human DNA polymerase 1 in *E. coli* and characterization of the recombinant enzyme. *Genes Cells* **7**, 639–651.
- Singhal, R.K. & Wilson, S.H. (1993) Short gap-filling synthesis by DNA polymerase  $\beta$  is processive. *J. Biol. Chem.* **268**, 15906–15911.
- Sobol, R.W., Horton, J.K., Kuhn, R., *et al.* (1996) Requirement of mammalian DNA polymerase- $\beta$  in base-excision repair. *Nature* **379**, 183–186.
- Soltis, D.A. & Uhlenbeck, O.C. (1982) Isolation and characterization of two mutant forms of T4 polynucleotide kinase. *J. Biol. Chem.* **257**, 11332–11339.

- Sugo, N., Aratani, Y., Nagashima, Y., Kubota, Y. & Koyama, H. (2000) Neonatal lethality with abnormal neurogenesis in mice deficient in DNA polymerase  $\beta$ . *EMBO J.* **19**, 1397–1404.
- Tamai, K., Kojima, K., Hanaichi, T., *et al.* (1988) Structural study of immunoaffinity-purified DNA polymerase  $\alpha$ -DNA primase complex from calf thymus. *Biochim. Biophys. Acta* **950**, 263–273.
- Tamiya-Koizumi, K., Murate, T., Suzuki, M., *et al.* (1997) Inhibition of DNA primase by sphingosine and its analogues parallels with their growth suppression of cultured human leukemic cells. *Biochem. Mol. Biol. Int.* **41**, 1179–1189.
- Uchiyama, Y., Kimura, S., Yamamoto, T., Ishibashi, T. & Sakaguchi, K. (2004) Plant DNA polymerase 1, a DNA repair enzyme that functions in plant meristematic and meiotic tissues. *Eur. J. Biochem.* **271**, 2799–2807.
- Usui, T., Watanabe, H., Nakayama, H., *et al.* (2004) The anticancer natural product pironetin selectively targets Lys352 of  $\alpha$ -tubulin. *Chem. Biol.* **11**, 799–806.
- Zhang, X., Morera, S., Bates, P.A., *et al.* (1998) Structure of an XRCC1 BRCT domain: a new protein–protein interaction module. *EMBO J.* **17**, 6404–6411.

Received: 25 October 2005

Accepted: 29 November 2005

## Supplementary material

The following supplementary material is available for this article online.

**Scheme 1** Synthesis of curcumin derivatives.